



Supporting Information

© Wiley-VCH 2007

69451 Weinheim, Germany

Multicomponent Cylindrical Assemblies Driven by Amidinium-Carboxylate Salt Bridge Formation: Salt Bridge and Guest-Encapsulation Induced Helical Twist

Hiroshi Katagiri,¹ Yoshie Tanaka,¹ Yoshio Furusho,^{1,*} and Eiji Yashima^{1,2,*}

¹Yashima Super-structured Helix Project, Exploratory Research for Advanced Technology (ERATO), Japan Science and Technology Agency (JST), Creation Core Nagoya 101, 2266-22 Shimoshidami, Moriyama-ku, Nagoya 463-0003, Japan.

²Institute for Advanced Research, Nagoya University, Chikusa-ku, Nagoya 464-8601, Japan.

*To whom correspondence should be addressed. E-mail: furusho@yp-jst.jp (Y.F.); yashima@apchem.nagoya-u.ac.jp (E.Y.)

Table of Contents

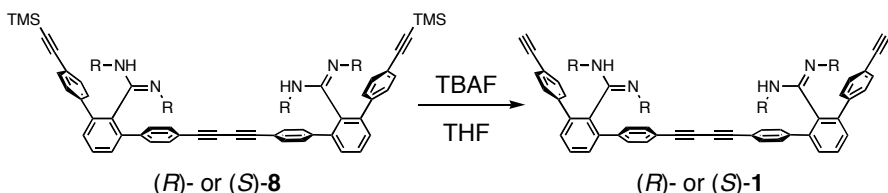
1. Instruments	S2
2. Materials and Methods	S2
3. Characterization of the Cylindrical Complexes (<i>R</i>)- 3 , (<i>R</i>)- 5 , and (<i>R</i>)- 5 -bipy	
ESI-MS Spectrum of the [3+2]Cylindrical Complex (<i>R</i>)- 3	S5
COSY and NOESY Spectra of the [3+2]Cylindrical Complex (<i>R</i>)- 3	S6
COSY and NOESY Spectra of the [4+2]Cylindrical Complex (<i>R</i>)- 5	S10
COSY Spectra of the Sandwich Complex (<i>R</i>)- 5 -bipy	S14
¹ H NMR Spectra of the [4+2]Cylindrical Complex (<i>R</i>)- 5	
with Various Amounts of bipy	S16
¹ H NMR Spectra of the Sandwich Complex (<i>R</i>)- 5 -bipy	
at Various Temperatures	S19
Proportion of the Sandwich Complex (<i>R</i>)- 5 -bipy	
to the Total Cylindrical Complexes	S22
X-ray Crystallographic Data of the [3+2]Cylindrical Complex (<i>S</i>)- 3	S23
Absorption and CD Spectra of the [3+2]Cylindrical Complex (<i>R</i>)- 3	
and the [4+2]Cylindrical Complex (<i>R</i>)- 5 at Various Temperatures	S26
Changes in the Absorption and CD Spectra of the [4+2]Cylindrical	
Complex (<i>R</i>)- 5 upon Addition of Pyridine	S27
4. References	S28

1. Instruments

Melting points were measured on a Yanaco MP-500 micro melting point apparatus and were uncorrected. NMR spectra were measured on a Varian UNITY INOVA 500AS spectrometer operating at 500 MHz for ^1H and at 125 MHz for ^{13}C . Absorption and CD spectra were measured by use of a Jasco V-570 spectrophotometer and a Jasco J-820 spectropolarimeter, respectively. Electron-spray ionization mass (ESI-MS) and cold-spray ionization mass (CSI-MS) spectra were recorded on a JEOL JMS-T100CS mass spectrometer. The single-crystal X-ray data for the [3+2]cylindrical complex (S)-3 were collected on a Bruker Smart Apex CCD-based X-ray diffractometer with Mo-K α radiation ($\lambda = 0.71073 \text{ \AA}$), and the structure was solved using the SHELXTL-PC crystallographic software package.^[1] Molecular modeling and molecular mechanics (MM) calculations were performed on a Windows XP PC with the Materials Studio package (Version 3.0; Accelrys Inc.).

2. Materials and Methods

All starting materials were purchased from commercial suppliers and were used without further purification unless otherwise noted. The diamidines (R)- and (S)-1 ((R,R,R,R)-1,4-bis(4"-ethynyl-2'-(N,N'-bis(1-phenylethyl)amidino)-1,1':3',1"-terphenyl)butadiyne) were prepared by treatment of diamidines (R)- and (S)-8^[2a] with tetra-*n*-butylammonium fluoride.^[2b] Zinc(II) 5,10,15,20-tetrakis(4-carboxyphenyl)porphyrin 4^[3] and monoamidines (R)- and (S)-6^[2b] were prepared according to the literature.



R = (R)-1-phenylethyl for (R)-1 and (R)-8; (S)-1-phenylethyl for (S)-1 and (S)-8.

Diamidines (R)- and (S)-1: To a solution of (R)-8 (355 mg, 0.290 mmol) in THF (20 mL) was added a solution of tetra-*n*-butylammonium fluoride (TBAF, 44 mg, 0.14 mmol) in THF (2.0 mL), and the resultant mixture was evaporated to dryness. The

residue was purified by column chromatography (NH-SiO₂, *n*-hexane/ether = 1/1) to give (*R*)-**1** as a white solid (291 mg, 95% yield). M.p. = 120–121 °C; ¹H NMR (500 MHz, CDCl₃, (*R*)-**1** (10.0 mM), CH₃CO₂H (66 mM), 25 °C): δ 13.03 (br s, 4H, NH), 7.77 (t, *J* = 7.7 Hz, 2H, ArH), 7.52 (d, *J* = 7.7 Hz, 4H, ArH), 7.32–7.21 (m, 20H, ArH), 7.03 (d, *J* = 7.1 Hz, 8H, ArH), 6.69 (d, *J* = 8.5 Hz, 4H, ArH), 6.68 (d, *J* = 8.5 Hz, 4H, ArH), 3.91 (m, 4H, CHN), 3.12 (s, 2H, CCH), 2.10 (s, 20H, CH₃CO₂), 0.72 (d, *J* = 6.6 Hz, 6H, CH₃CHN), 0.71 (d, *J* = 6.9 Hz, 6H, CH₃CHN); ¹³C NMR (125 MHz, CDCl₃, (*R*)-**1** (10.0 mM), CH₃CO₂H (66 mM), 25 °C): δ 177.14, 162.51, 142.45, 141.53, 141.35, 138.73, 138.27, 132.81, 132.44, 132.00, 130.71, 130.57, 129.09, 129.06, 128.63, 128.50, 128.06, 128.01, 126.54, 122.41, 122.37, 121.89, 82.76, 81.35, 78.82, 75.34, 55.52, 22.04, 22.01; FT-IR (KBr): ν 3426 (N–H), 3294 (C≡C–H), 2213 (C≡C), 2107 (C≡C), 1637 (C≡N) cm^{−1}; Anal. Calcd. for C₇₈H₆₂N₄: C, 88.77; H, 5.92; N, 5.31. Found: C, 88.55; H, 5.93; N, 5.10. In a similar manner, (*S*)-**1** was prepared from (*S*)-**8**. The ¹H NMR spectrum of (*S*)-**1** was virtually the same as that of (*R*)-**1**.

[3+2]Cylindrical Complex (*R*)-3**:** To a solution of **2** (2.52 mg, 12.0 μmol) in THF (0.5 mL) was added a solution of (*R*)-**1** (19.0 mg, 18.0 μmol) in CHCl₃ (1.1 mL). The resulting solution was evaporated to dryness to yield (*R*)-**3** as a white solid. M.p. = 210–212 °C; ¹H NMR (500 MHz, CDCl₃, 1.0 mM, 25 °C): δ 14.71 (br s, 12H, NH), 9.13 (s, 6H, ArH), 7.70 (t, *J* = 7.5 Hz, 6H, ArH), 7.45 (t, *J* = 7.5 Hz, 12H, ArH), 7.39 (t, *J* = 7.3 Hz, 12H, ArH), 7.33–7.25 (m, 34H, ArH), 7.21 (d, *J* = 8.2 Hz, 18H, ArH), 7.15 (t, *J* = 7.3 Hz, 22H, ArH), 6.64 (d, *J* = 8.2 Hz, 22H, ArH), 3.93 (m, 12H, CHN), 3.10 (s, 6H, C≡CH), 0.844 (d, *J* = 6.9 Hz, 18H, CH₃CHN), 0.840 (d, *J* = 6.6 Hz, 18H, CH₃CHN); FT-IR (KBr): ν 3424 (N–H), 3295 (C≡C–H), 2214 (C≡C), 2107 (C≡C), 1634 (C≡N) cm^{−1}; ESI-MS (+) (see Figure S1a): m/z = 3586.74 [M+H]⁺, 1793.74 [M+2H]²⁺; Anal. Calcd. for C₂₅₂H₁₉₈N₁₂O₁₂: C, 84.40; H 5.56; N, 4.69. Found: C, 84.43; H, 5.80; N, 4.51. In a similar manner, (*S*)-**3** was prepared from (*S*)-**1** and **2**. ¹H NMR (500 MHz, CDCl₃, 1.0 mM, 25 °C): δ 14.71 (br s, 12H, NH), 9.13 (s, 6H, ArH), 7.70 (t, *J* = 7.5 Hz, 6H, ArH), 7.45 (t, *J* = 7.5 Hz, 12H, ArH), 7.39 (t, *J* = 7.3 Hz, 12H, ArH), 7.33–7.25 (m, 34H, ArH), 7.21 (d, *J* = 8.2 Hz, 18H, ArH), 7.15 (t, *J* = 7.3 Hz, 22H, ArH), 6.64 (d, *J* = 8.2 Hz, 22H, ArH), 3.93 (m, 12H, CHN), 3.10 (s, 6H, C≡CH), 0.844

(d, $J = 6.9$ Hz, 18H, CH_3CHN), 0.840 (d, $J = 6.6$ Hz, 18H, CH_3CHN).

[4+2]Cylindrical Complex (*R*)-5: (*R*)-5 was prepared by stirring a mixture of (*R*)-1 (4.22 mg, 4.00 μ mol) and 4 (1.71 mg, 2.00 μ mol) in $CDCl_3$ (750 μ L) at ambient temperature for 12 h. CSI-MS (–) (see Figure S1b): $m/z = 5959.61$ [$M-H+MeOH$][–], 3000.54 [$M-4+Cl$][–]; 1H NMR (500 MHz, $CDCl_3$, 0.1 mM, 25 °C): δ 9.19 (s, 8H), 8.90 (s, 8H), 8.57 (d, $J = 7.9$ Hz, 8H), 8.55 (d, $J = 7.9$ Hz, 8H), 8.28 (d, $J = 7.7$ Hz, 8H), 8.25 (d, $J = 7.9$ Hz, 8H), 7.81 (t, $J = 7.9$ Hz, 8H), 7.59 (d, $J = 7.5$ Hz, 8H), 7.55 (d, $J = 7.5$ Hz, 8H), 7.40–7.27 (m, 112H), 6.88–6.80 (m, 32H), 4.11–4.01 (m, 16H), 3.17 (s, 8H), 1.01 (d, $J = 6.6$ Hz, 24H), 0.92 (d, $J = 6.6$ Hz, 24H). (*R*)-5 was further characterized by its COSY and NOESY spectra, which unambiguously support its cylindrical structure as well as purity (see Figures S6–S9).

[4+1]Cylindrical Complex (*R*)-7: (*R*)-7 was prepared by stirring a mixture of amidine (*R*)-6 (4.88 mg, 9.23 μ mol) and 4 (1.97 mg, 2.31 μ mol) in $CDCl_3$ (5.0 mL) at ambient temperature for 12 h. 1H NMR (500 MHz, $CDCl_3$, 0.1 mM, 25 °C): δ 14.10 (s, 8H), 9.05 (s, 8H), 8.56 (d, $J = 7.9$ Hz, 8H) 8.30 (d, $J = 7.9$ Hz, 8H), 7.80 (t, $J = 7.7$ Hz, 4H), 7.57 (d, $J = 7.7$ Hz, 8H), 7.37–7.25 (m, 56H), 6.80 (d, $J = 8.3$ Hz, 16H), 4.03 (m, 8H), 3.15 (s, 8H), 0.91 (d, $J = 6.7$ Hz, 24H).

Molecular Mechanics (MM) Calculation: The MM calculations were performed on a Windows XP PC with the Materials Studio package (Version 3.0; Accelrys Inc.). The geometry optimizations were carried out by the steepest descent, conjugated gradient and finally Quasi-Newton methods (smart algorism) with the Forcite program using the Dreiding force field. The energy minimization was continued until the total energy change became less than 0.002 kcal mol^{–1}.

3. Characterization of the Cylindrical Complexes (*R*)-3, (*R*)-5, and (*R*)-5-bipy

ESI-MS Spectrum of the Complex (*R*)-3 and (*R*)-5

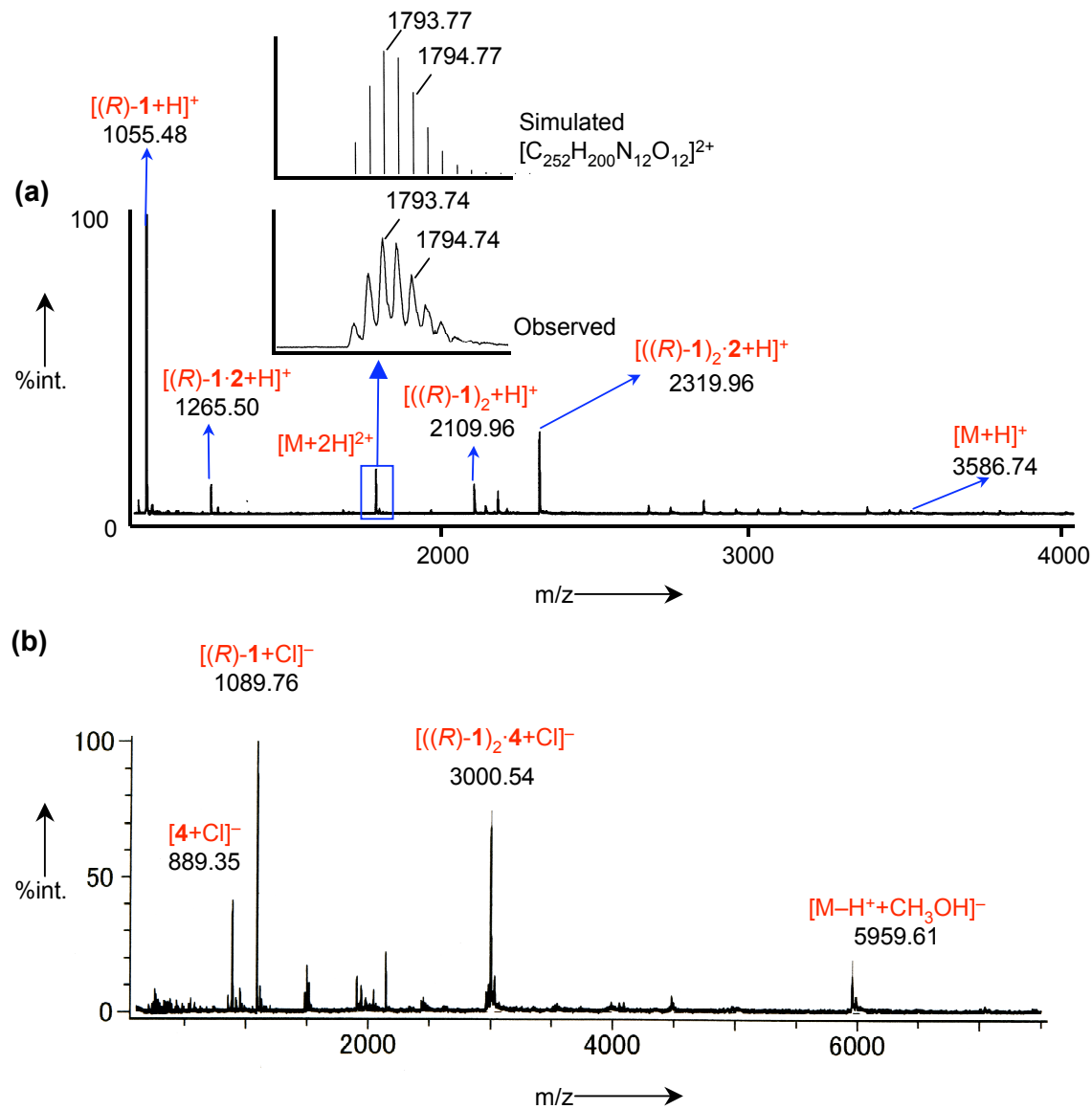


Figure S1. (a) Positive mode ESI-MS ($CHCl_3/MeOH = 10/1$ as a solvent) spectrum of the $[3+2]$ cylindrical complex (*R*)-3. (b) Negative mode CSI-MS ($CHCl_3/MeOH = 10/1$ as a solvent; ion source temperature = -30 $^{\circ}C$; Ph_4PCl as a charge carrier^[4]) spectrum of the $[4+2]$ cylindrical complex (*R*)-5.

COSY and NOESY Spectra of the [3+2]Cylindrical Complex (*R*)-3
COSY Spectra of the [3+2]Cylindrical Complex (*R*)-3

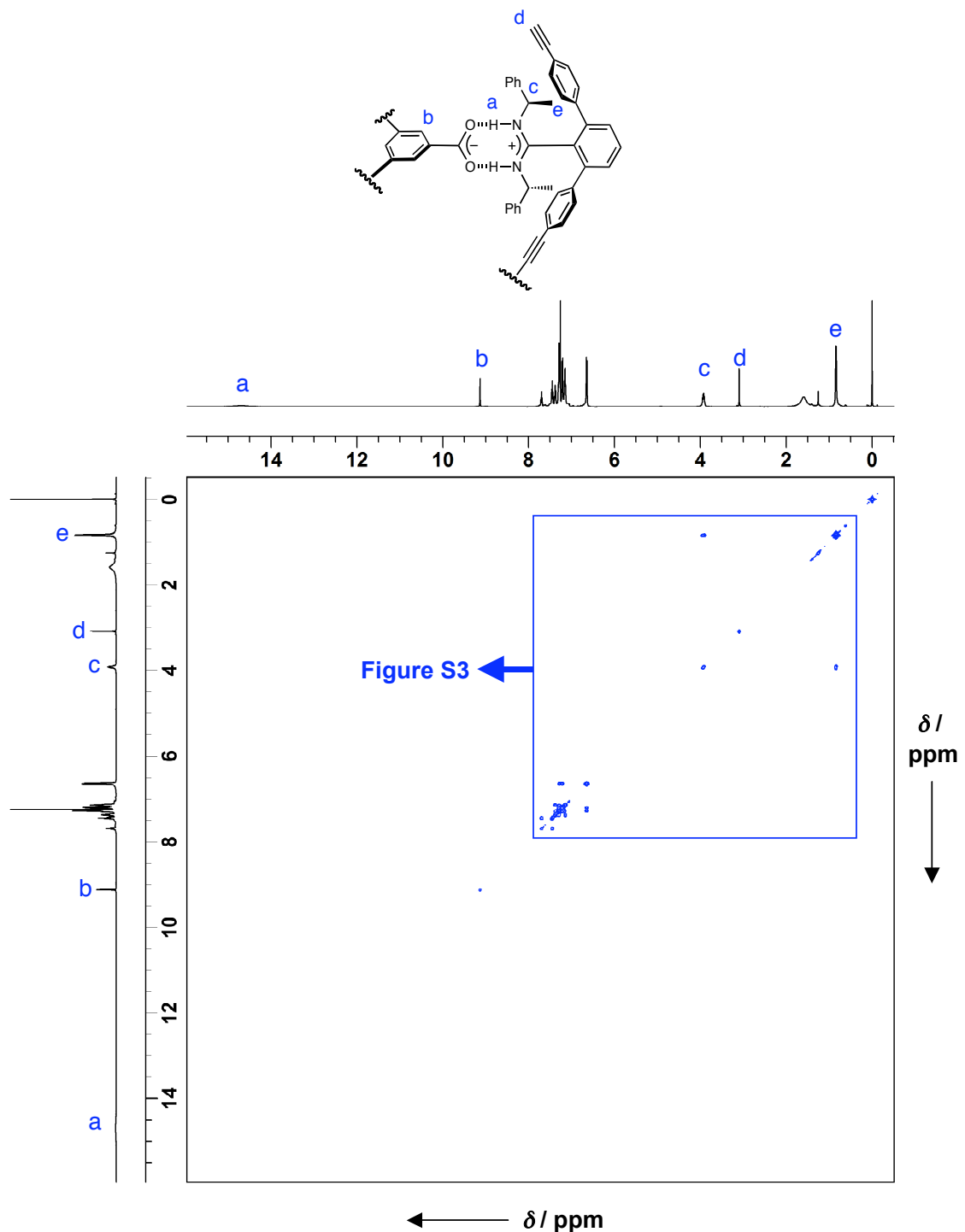


Figure S2. 500 MHz COSY spectrum of the cylindrical complex (*R*)-3 in CDCl_3 (0.1 mM) at 25 °C.

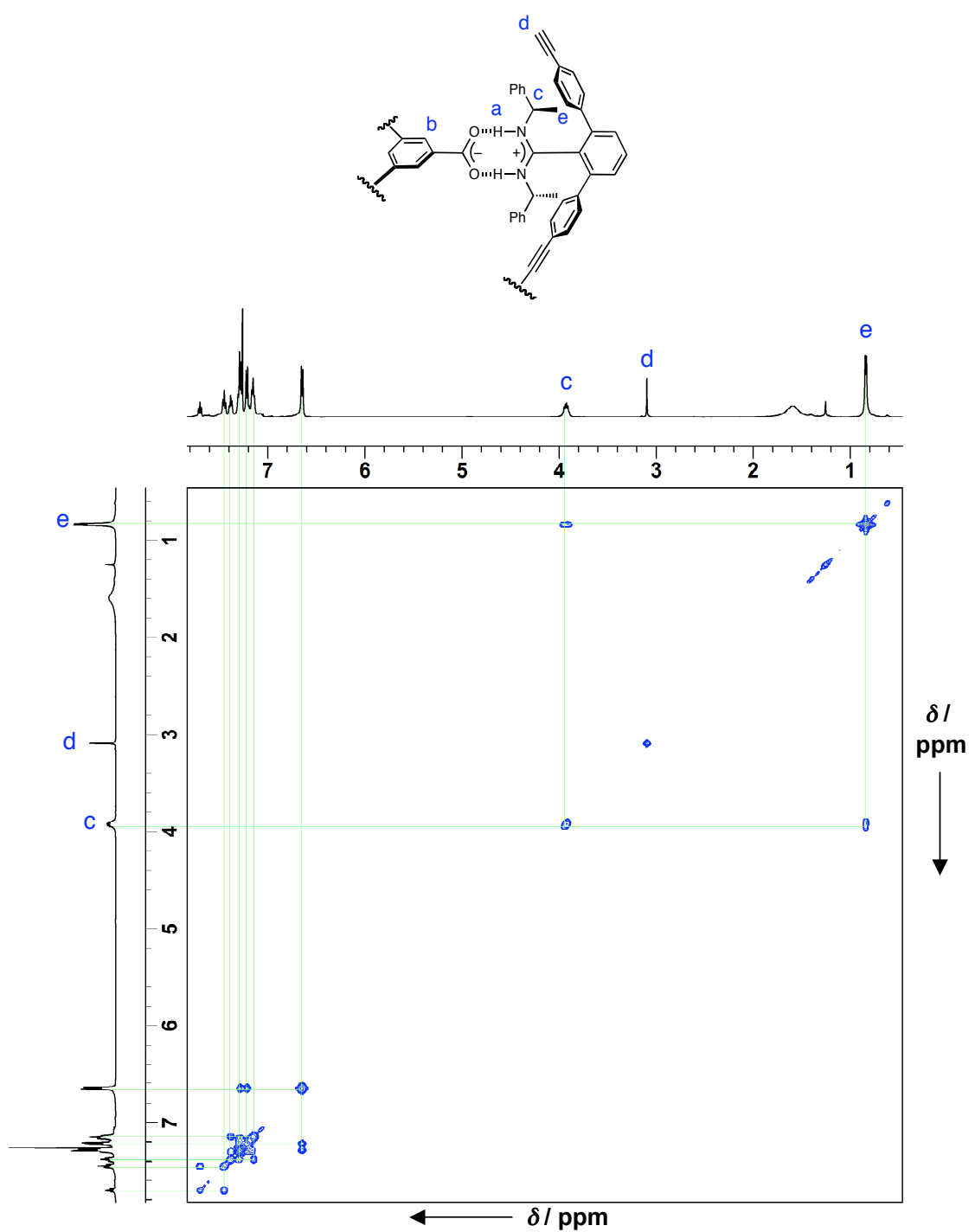


Figure S3. Partial 500 MHz COSY spectrum of the cylindrical complex (R)-3 in CDCl_3 (0.1 mM) at 25 °C.

NOESY Spectra of the [3+2]Cylindrical Complex (*R*)-3

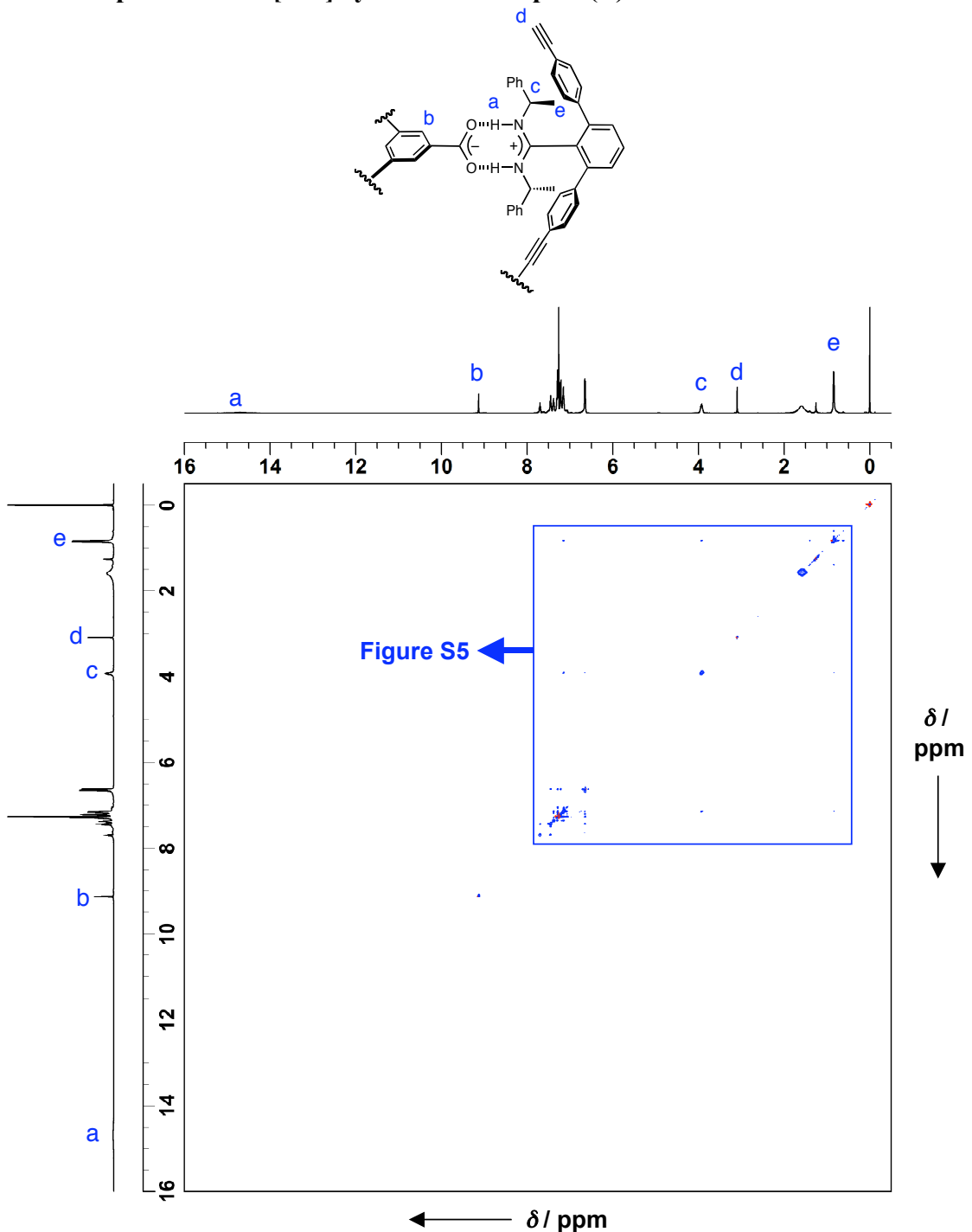


Figure S4. 500 MHz NOESY spectrum of the [3+2]cylindrical complex (*R*)-3 in CDCl_3 (0.1 mM) at 25 °C (mixing time = 300 ms).

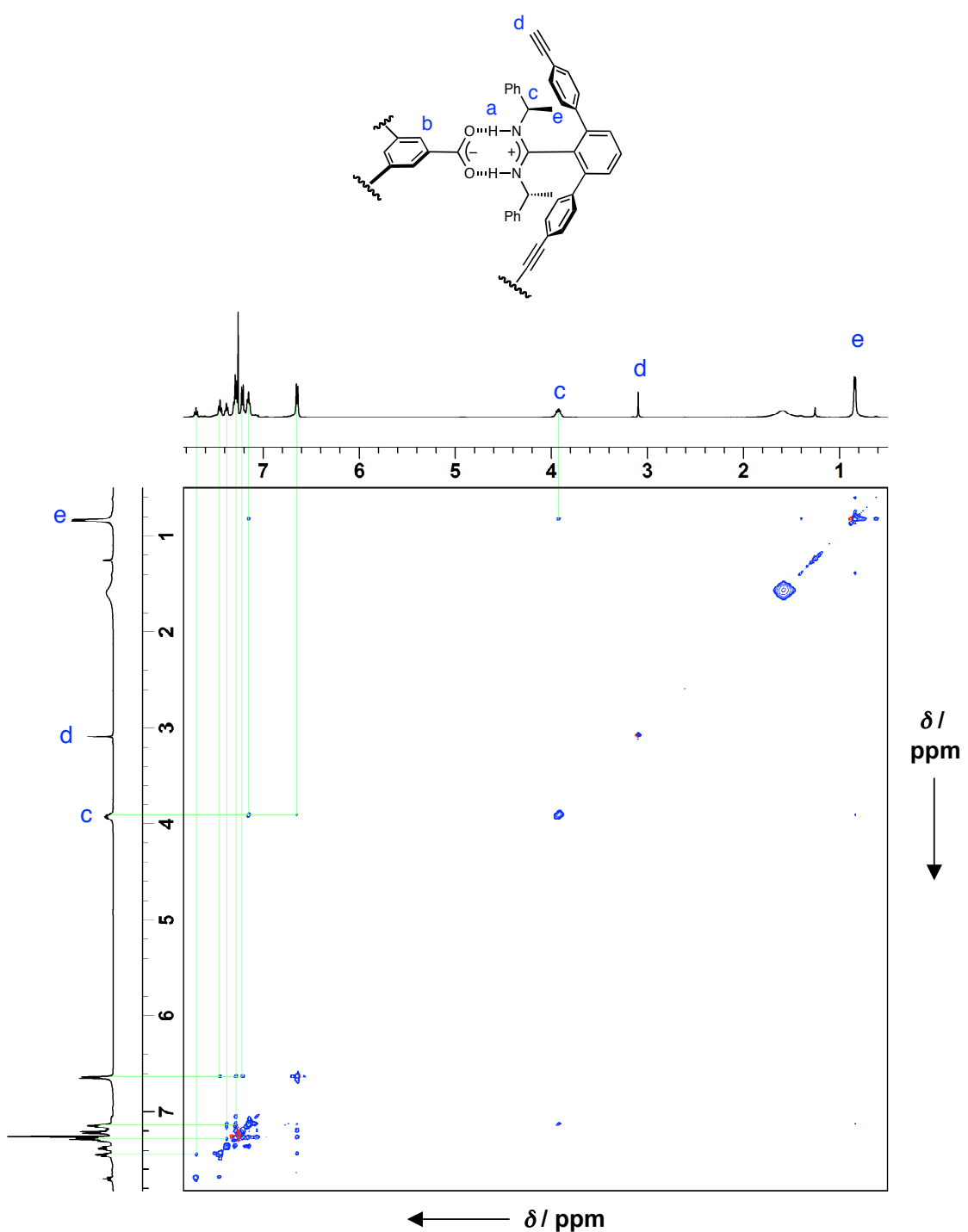


Figure S5. Partial 500 MHz NOESY spectrum of the [3+2]cylindrical complex (R)-3 in CDCl_3 (0.1 mM) at 25 °C (mixing time = 300 ms).

COSY and NOESY Spectra of the [4+2]Cylindrical Complex (*R*)-5
COSY Spectra of the [4+2]Cylindrical Complex (*R*)-5

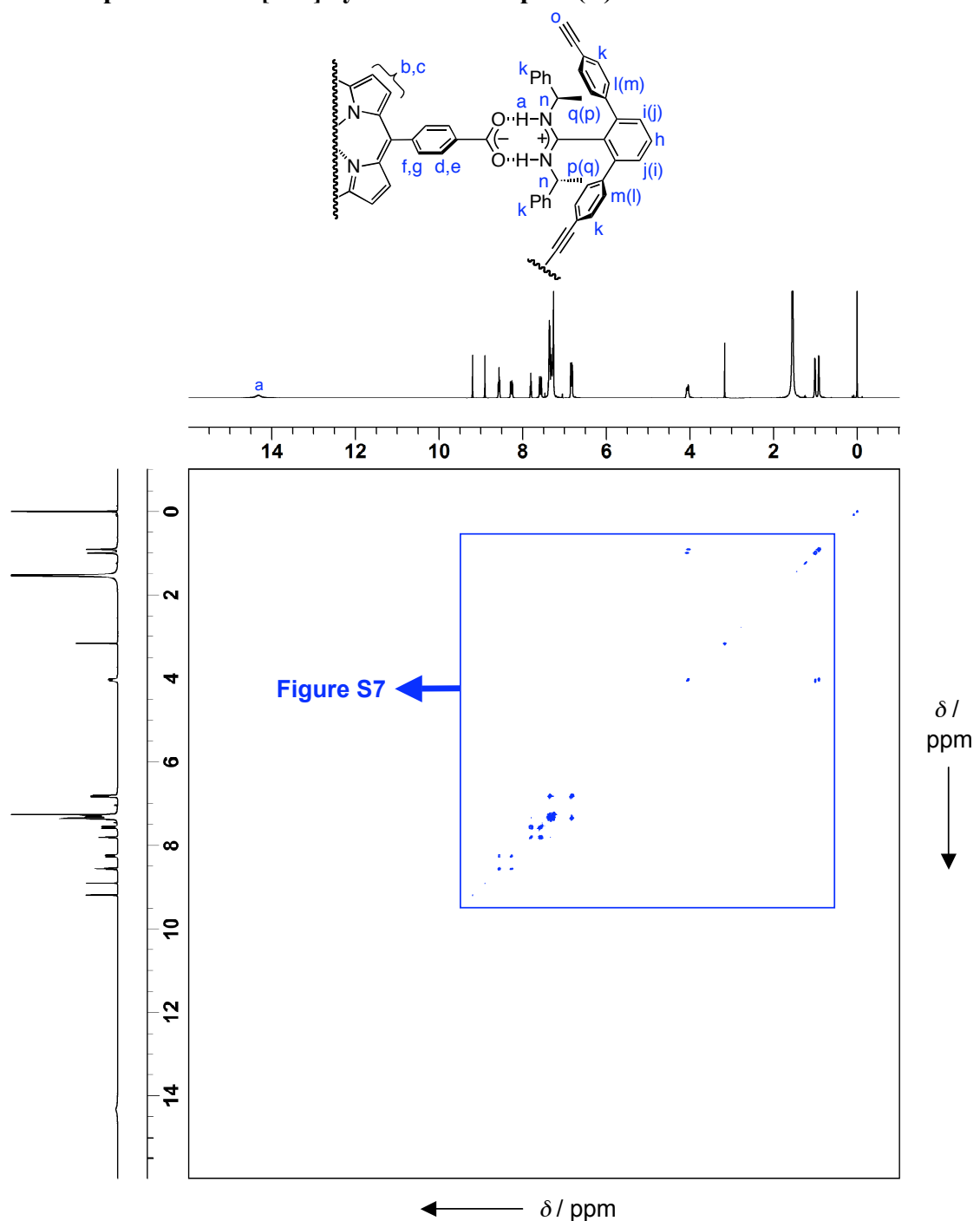


Figure S6. 500 MHz COSY spectrum of the [4+2]cylindrical complex (*R*)-5 in CDCl_3 (0.1 mM) at 25 °C.

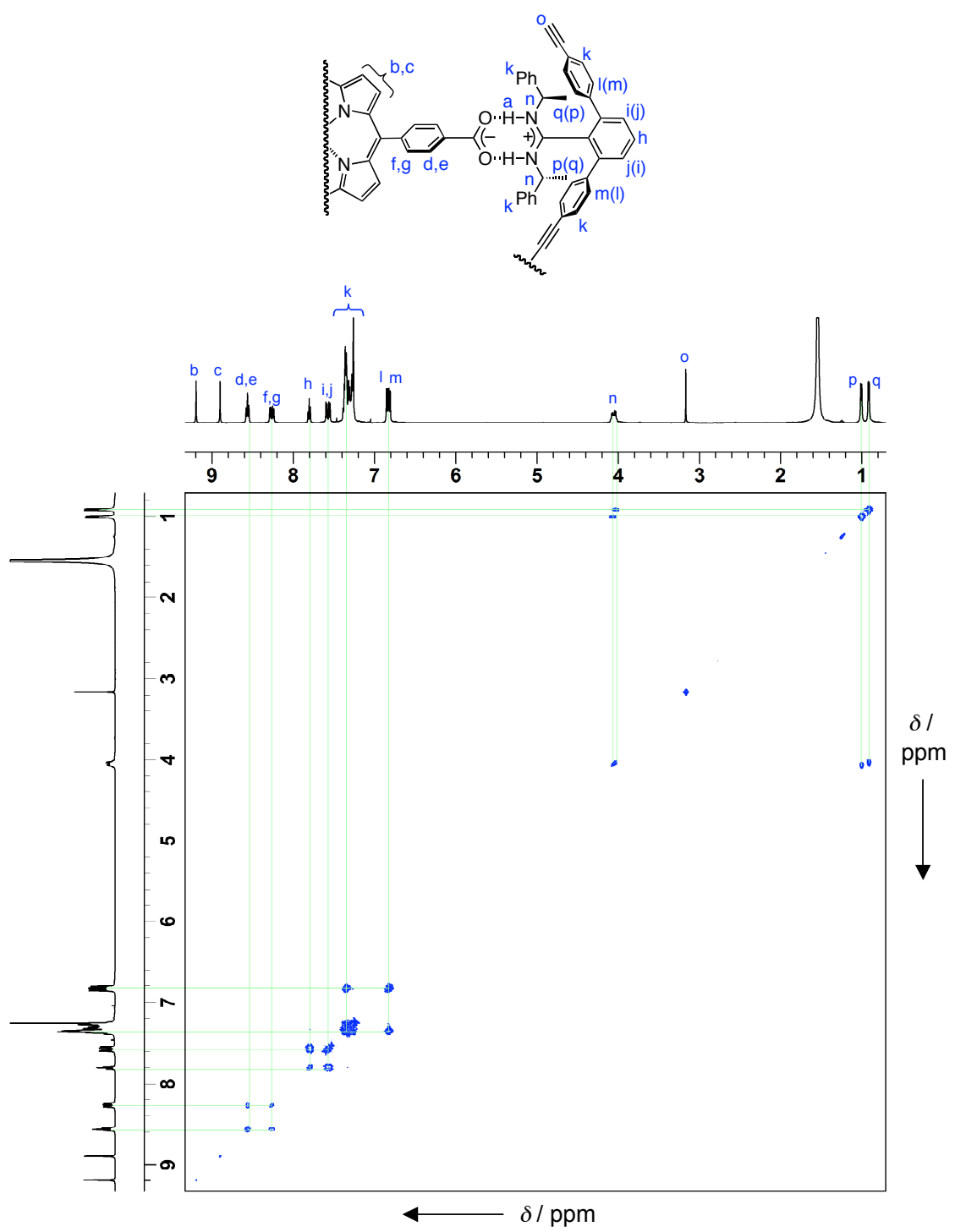


Figure S7. Partial 500 MHz COSY spectrum of the [4+2]cylindrical complex (*R*)-5 in CDCl_3 (0.1 mM) at 25 °C.

NOESY Spectra of the [4+2]Cylindrical Complex (R)-5

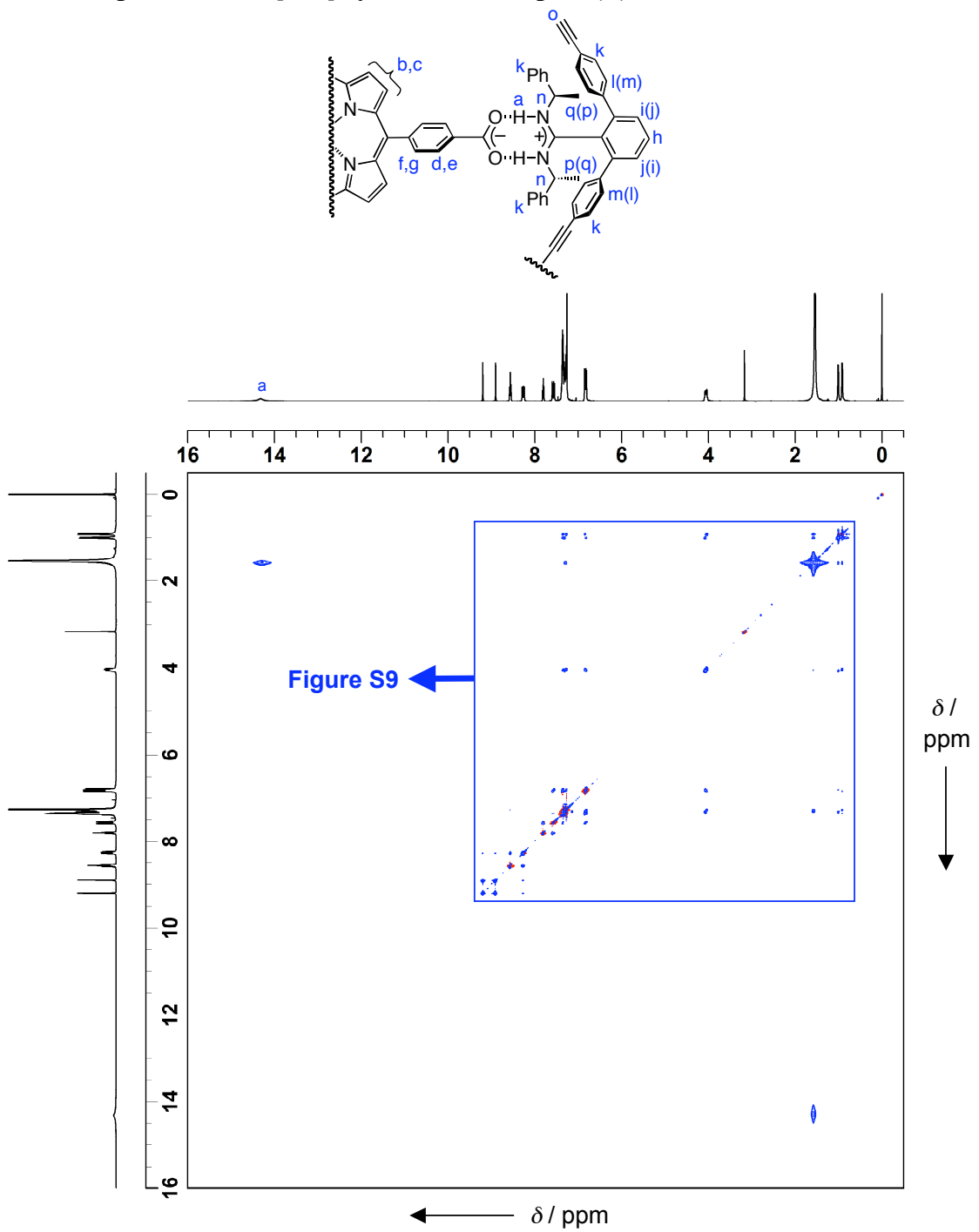


Figure S8. 500 MHz NOESY spectrum of the [4+2]cylindrical complex (R)-5 in CDCl_3 (0.1 mM) at 25 °C (mixing time = 300 ms).

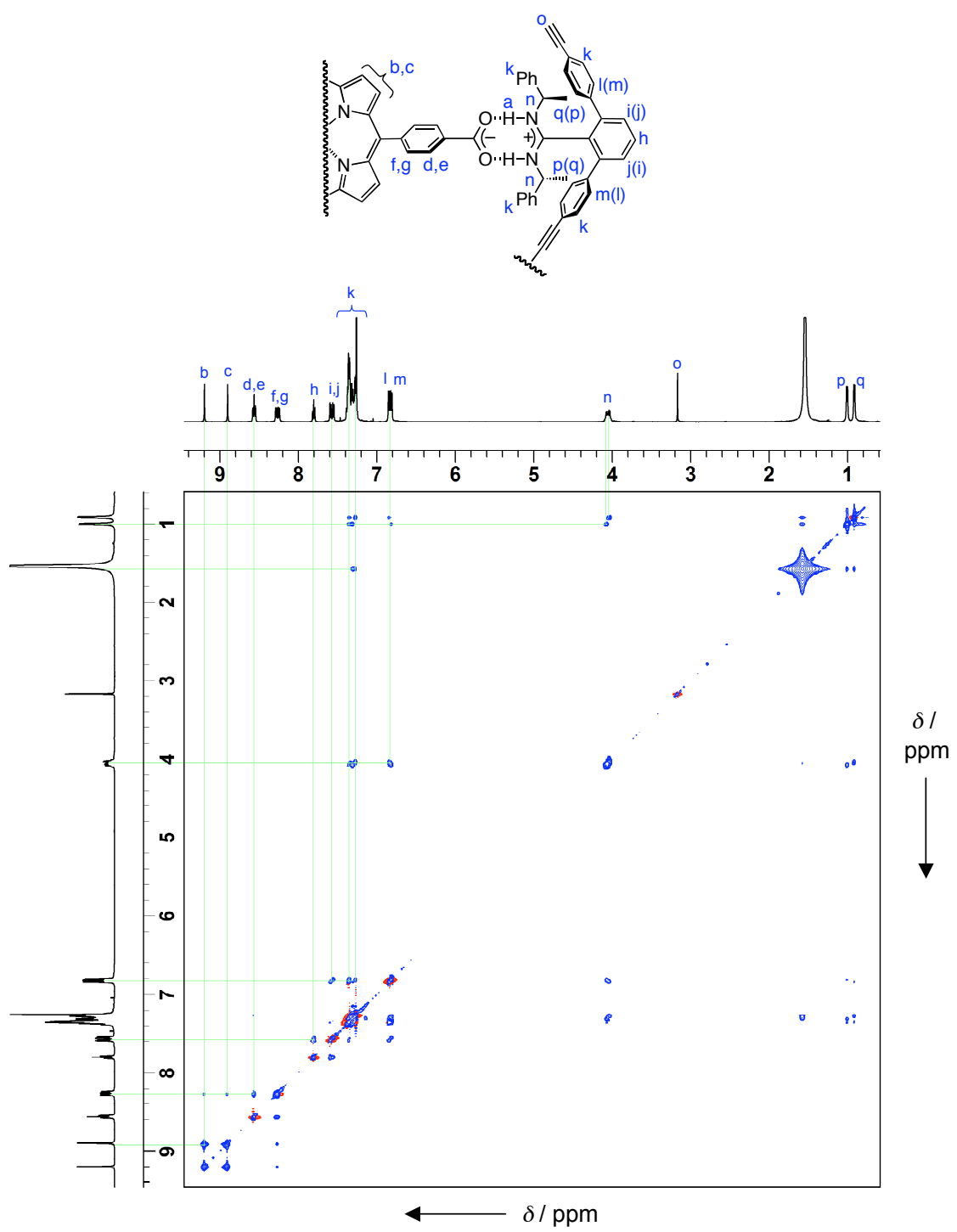


Figure S9. Partial 500 MHz NOESY spectrum of the [4+2]cylindrical complex (R)-5 in CDCl_3 (0.1 mM) at 25 °C (mixing time = 300 ms).

COSY Spectra of the Sandwich Complex *(R*)-5–bipy

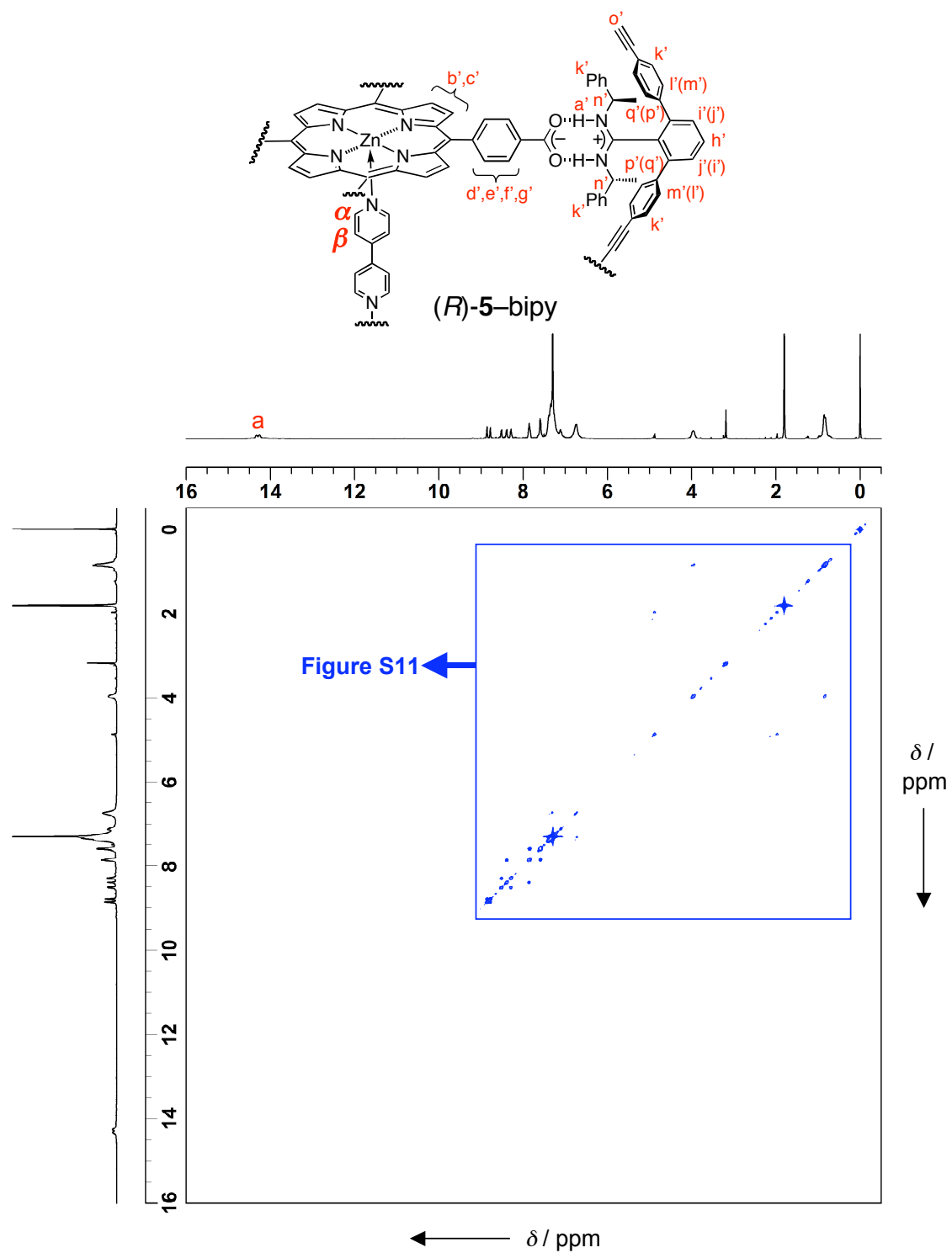


Figure S10. 500 MHz COSY spectrum of the sandwich complex *(R*)-5–bipy formed from **(R)-5** and an equimolar amount of bipy in CDCl_3 (0.1 mM) at -55°C .

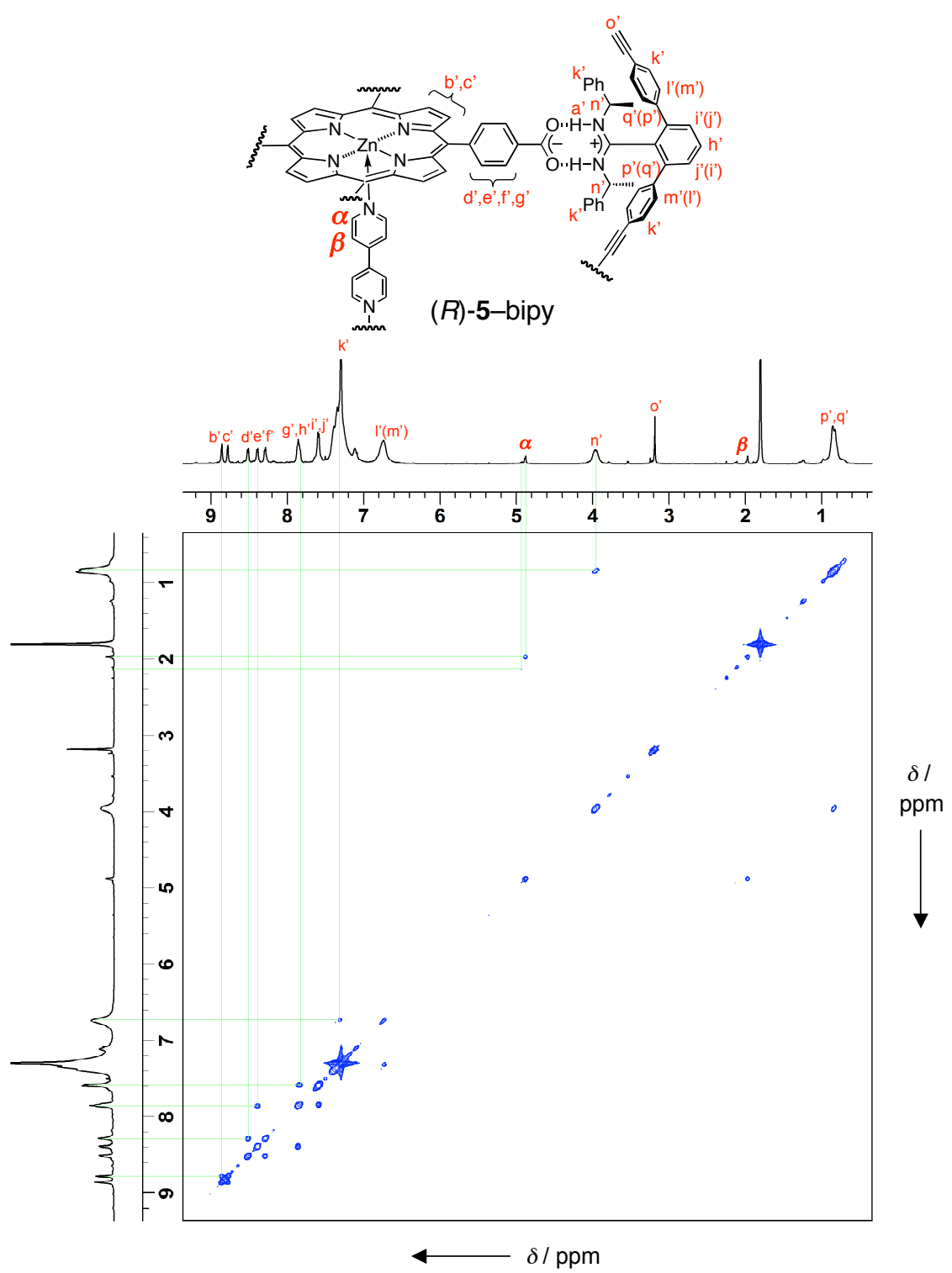


Figure S11. Partial 500 MHz COSY spectrum of the sandwich complex *(R)*-5-bipy formed from *(R)*-5 and an equimolar amount of bipy in CDCl_3 (0.1 mM) at -55°C .

^1H NMR Spectra of the [4+2]Cylindrical Complex (*R*)-5 with Various Amounts of bipy

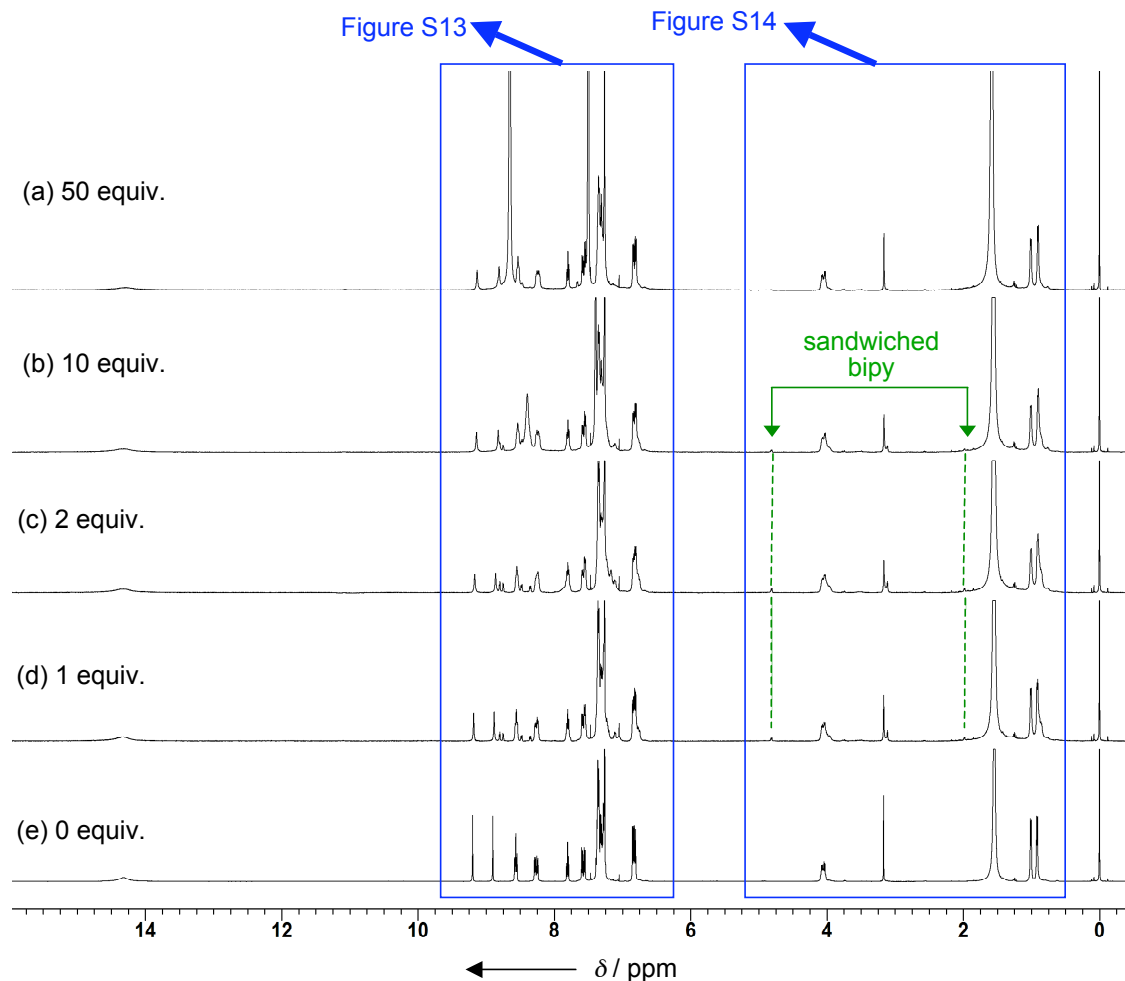


Figure S12. ^1H NMR spectra of the [4+2]cylindrical complex (*R*)-5 in the presence of (a) 50, (b) 10, (c) 2, (d) 1, and (e) 0 equiv. of bipy in CDCl_3 (0.1 mM) at 25 °C.

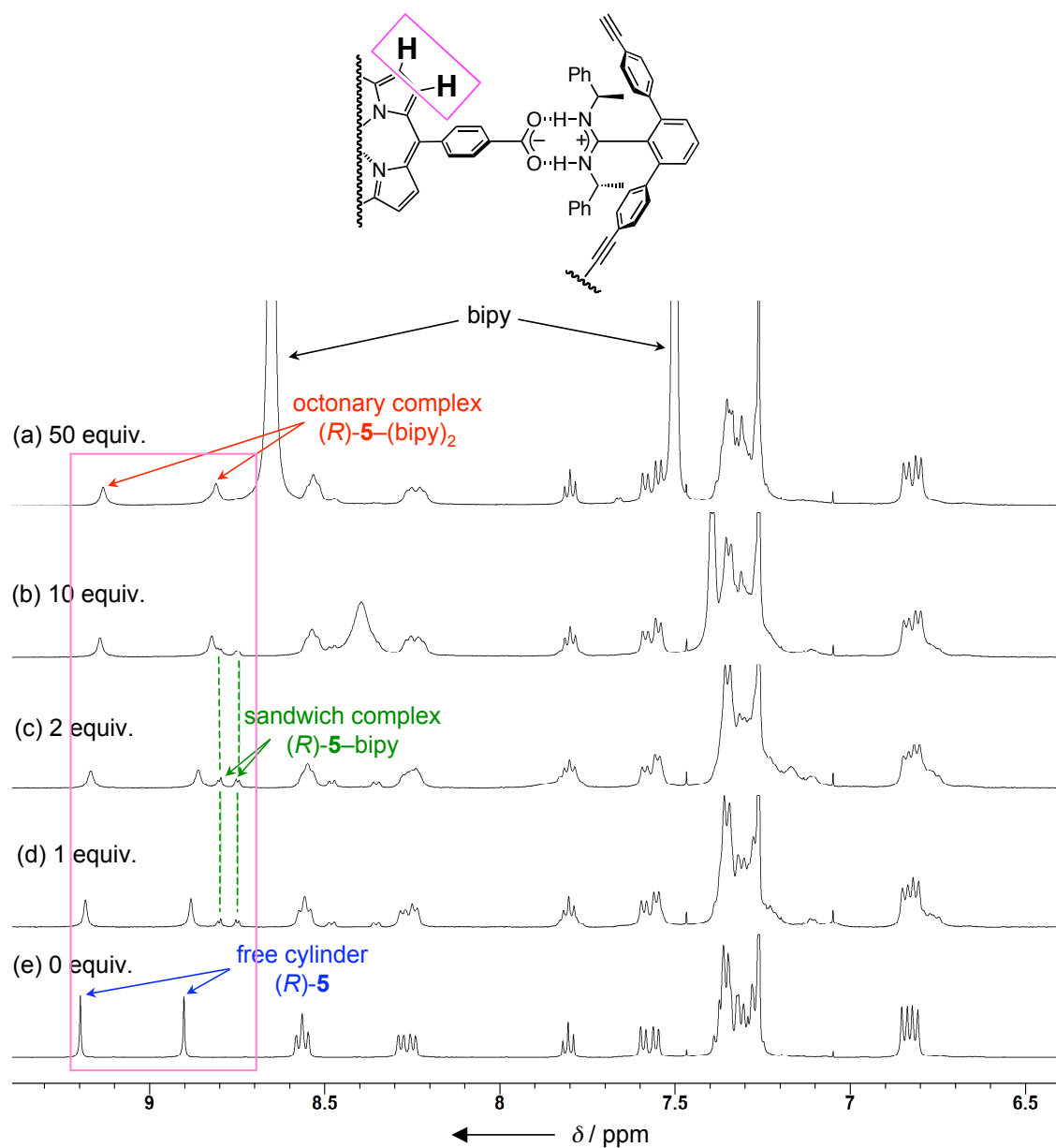


Figure S13. Partial ^1H NMR spectra of the [4+2]cylindrical complex (R)-5 in the presence of (a) 50, (b) 10, (c) 2, (d) 1, and (e) 0 equiv. of bipy in CDCl_3 (0.1 mM) at 25 $^{\circ}\text{C}$.

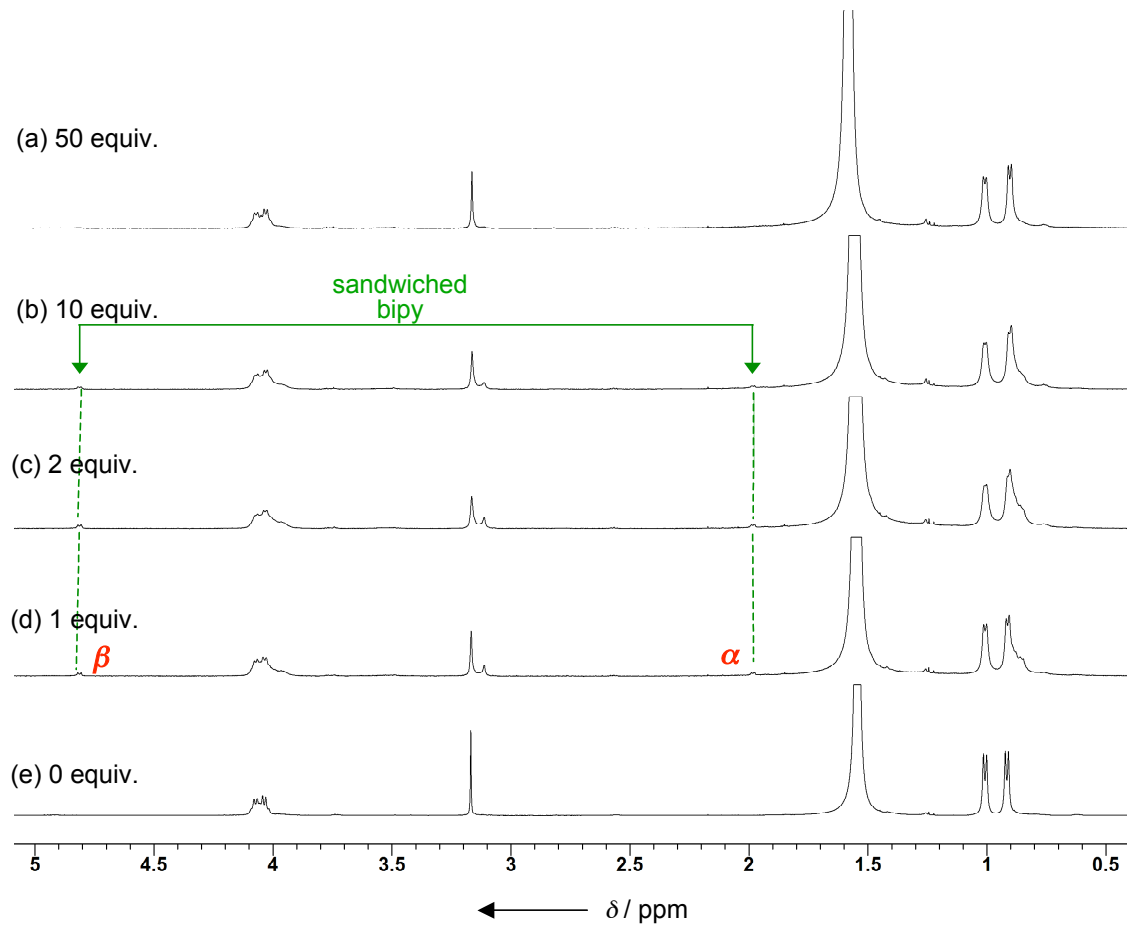
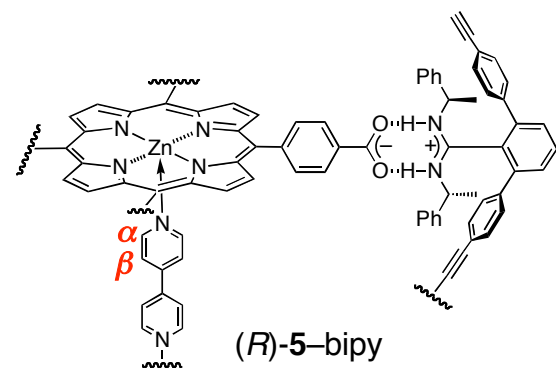


Figure S14. Partial ^1H NMR spectra of the [4+2]cylindrical complex (R)-5 in the presence of (a) 50, (b) 10, (c) 2, (d) 1, and (e) 0 equiv. of bipy in CDCl_3 (0.1 mM) at 25 $^\circ\text{C}$.

¹H NMR Spectra of the Sandwich Complex (R)-5-bipy at Various Temperatures

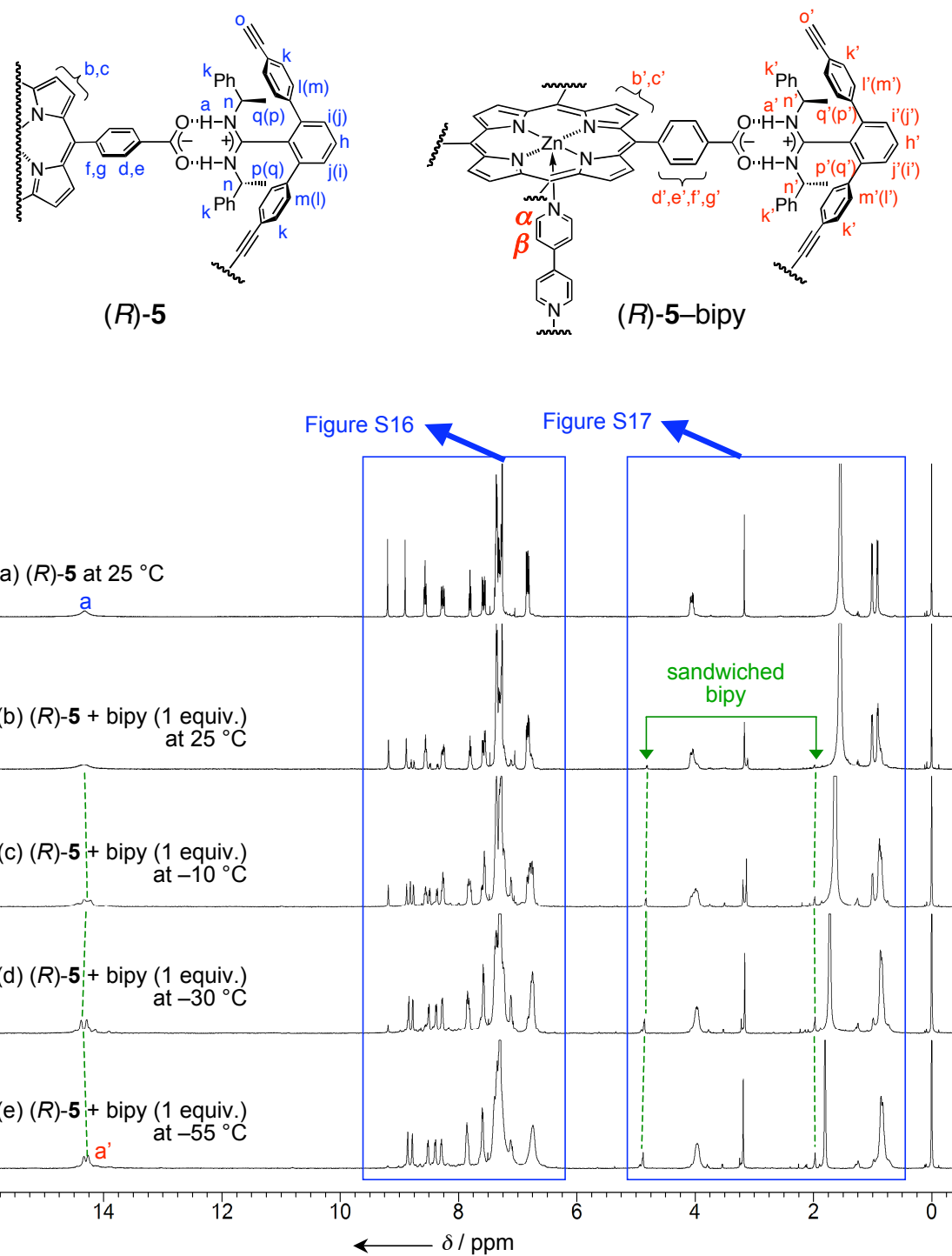


Figure S15. 500 MHz ¹H NMR spectra of (a) the [4+2]cylindrical complex (R)-5, (b) (R)-5 in the presence of an equimolar amount of bipy at 25, (c) -10, (d) -30, and (e) -55 °C in CDCl₃ (0.1 mM). The resonances due to free bipy and bipy of (R)-5-(bipy)₂ gave the averaged signals because of the fast exchange on the ¹H NMR time scale.

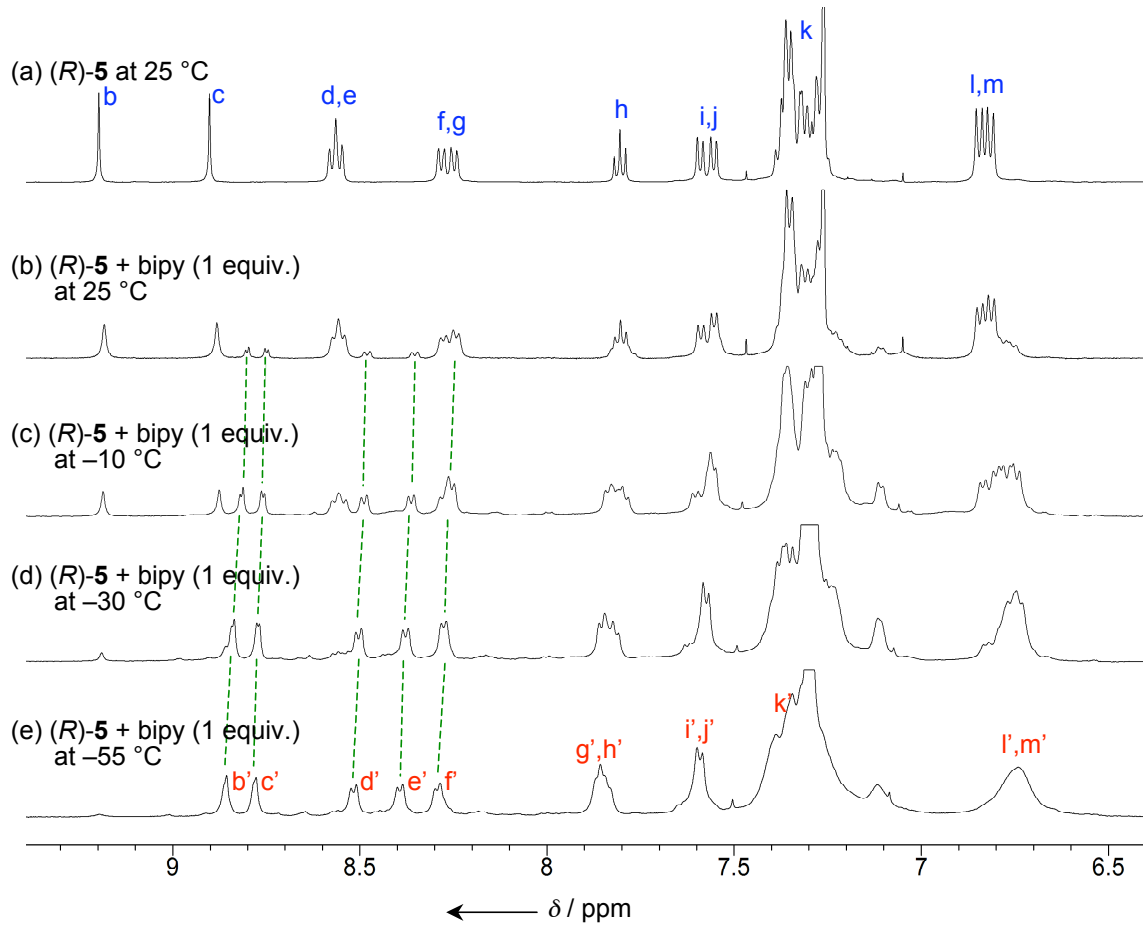
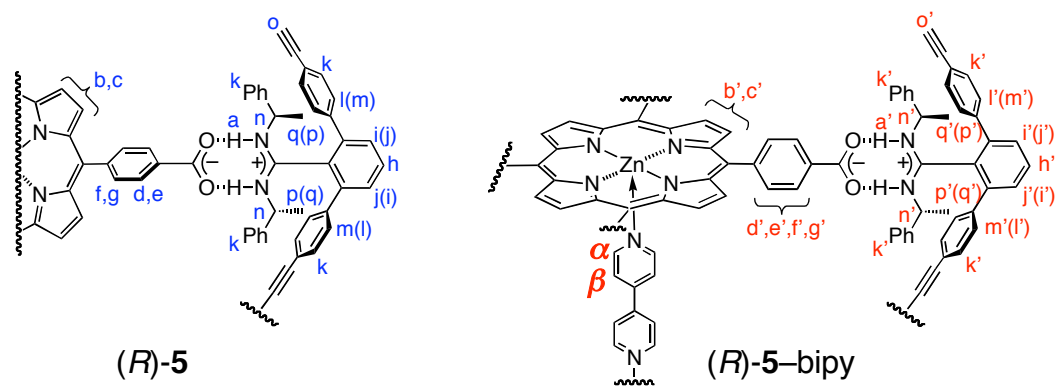


Figure S16. Partial 500 MHz ^1H NMR spectra of (a) the [4+2]cylindrical complex (R)-5, and (R)-5 in the presence of an equimolar amount of bipy at (b) 25, (c) -10, (d) -30, and (e) -55 °C in CDCl_3 (0.1 mM).

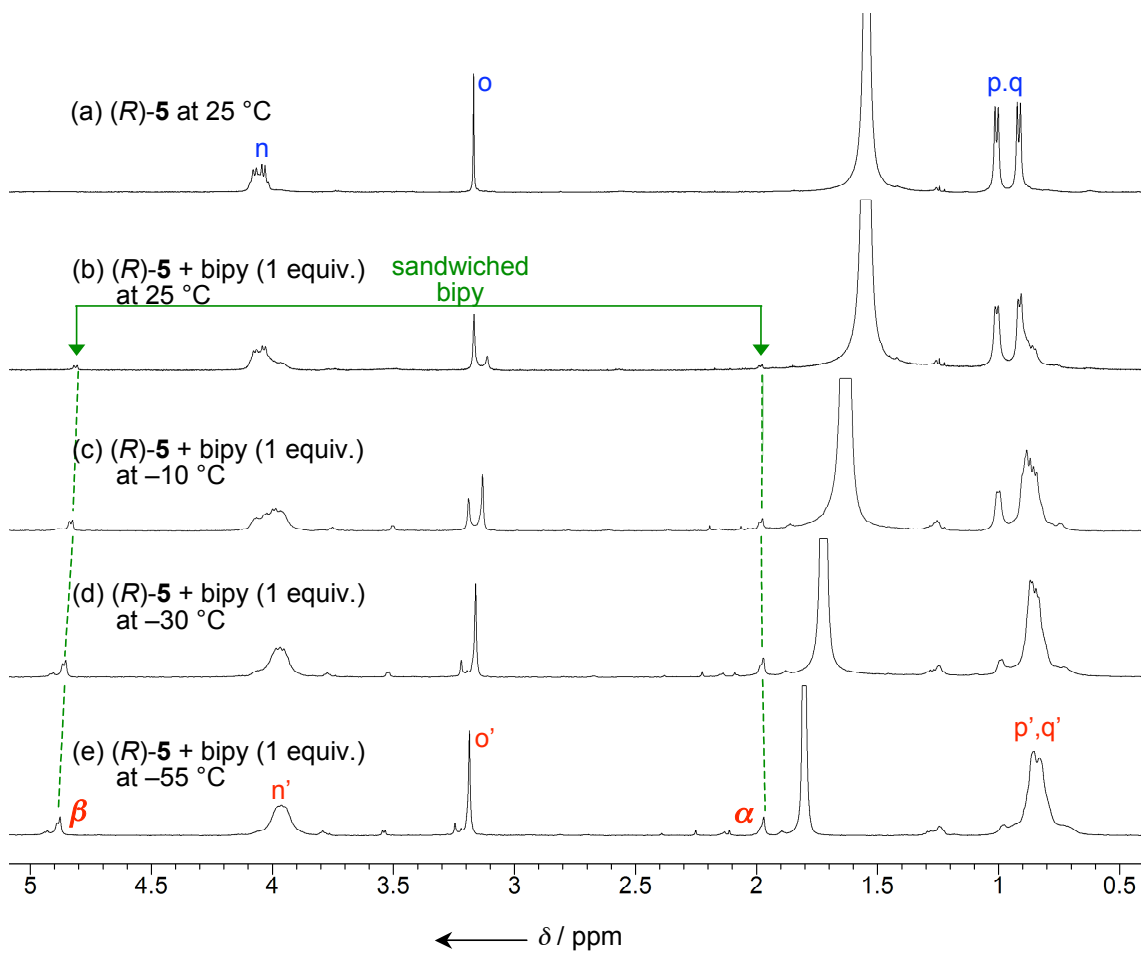
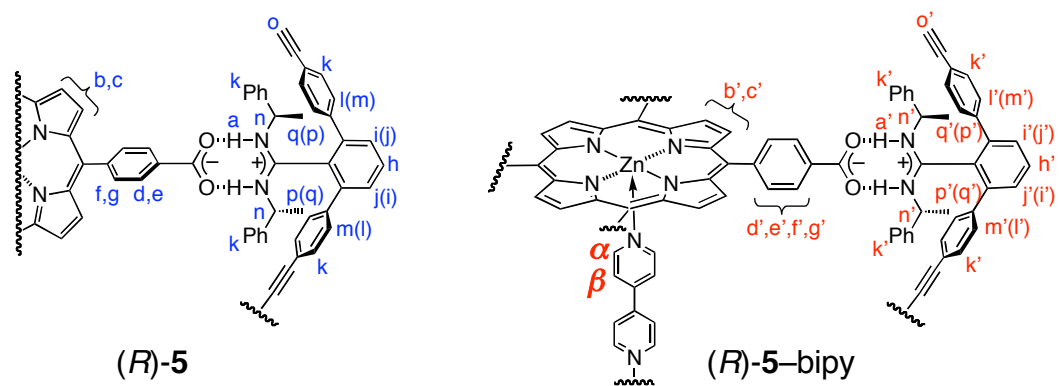


Figure S17. Partial 500 MHz ^1H NMR spectra of (a) the [4+2]cylindrical complex (*R*)-5, and (*R*)-5 in the presence of an equimolar amount of bipy at (b) 25, (c) -10, (d) -30, and (e) -55 °C in CDCl_3 (0.1 mM).

Proportion of the Sandwich Complex (*R*-5-bipy to the Total Cylindrical Complexes

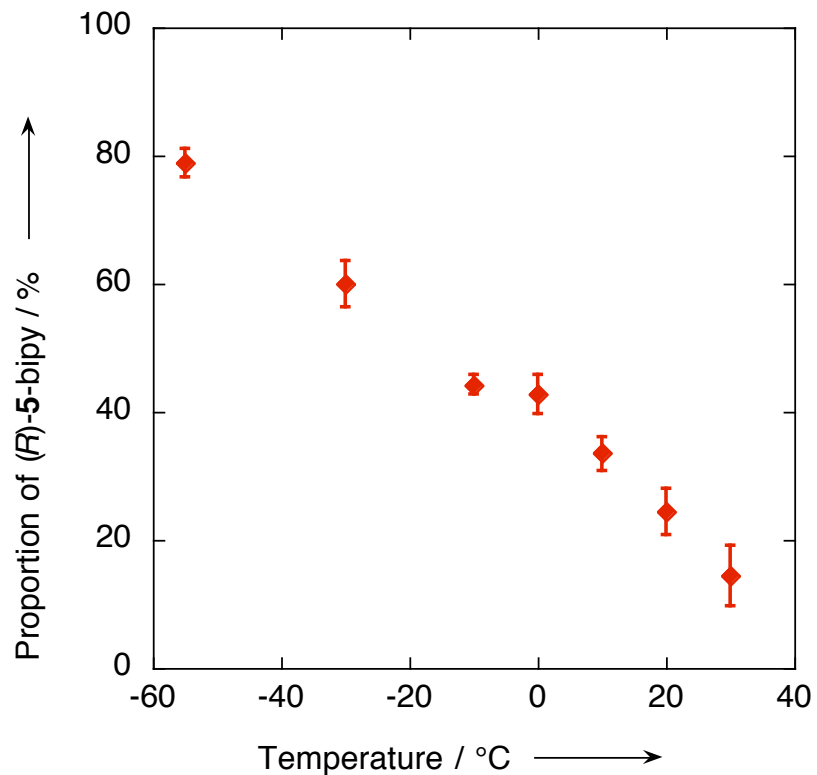


Figure S18. Changes in the proportion of (R)-5-bipy to the total cylindrical complexes in the presence of an equimolar amount of bipy at various temperatures. The proportion values were estimated from the integrals of the sandwiched bipy signals in their ^1H NMR spectra (see Figure S17 for examples).

X-ray Crystallographic Data of the Cylindrical Complex (S)-3

X-Ray diffraction data for the cylindrical complex (S)-3 were collected on a Bruker Smart Apex CCD-based X-ray diffractometer with Mo-K α radiation ($\lambda = 0.71073 \text{ \AA}$) at 153 K. Single crystals of (S)-3 ($\text{C}_{252}\text{H}_{218}\text{N}_{12}\text{O}_{12}$, Mw = 3766.57) suitable for X-ray analysis were grown by liquid diffusion of *n*-hexane into a chloroform solution of (S)-3, and a single colorless crystal with dimensions $0.30 \times 0.15 \times 0.05 \text{ mm}$ was selected for intensity measurements. The unit cell was monoclinic with the space group $P1$. Lattice constants with $Z = 1$, $\rho_{\text{calcd}} = 0.993 \text{ g cm}^{-3}$, $\mu(\text{Mo-K}\alpha) = 0.063 \text{ mm}^{-1}$, $F(000) = 1970$, and $2\theta_{\text{max}} = 50.7^\circ$ were $a = 17.395(2)$, $b = 18.235(3)$, $c = 22.228(3) \text{ \AA}$, $\alpha = 88.211(2)$, $\beta = 87.456(3)$, $\gamma = 63.587(3)^\circ$, and $V = 6307.9(15) \text{ \AA}^3$. A total of 32965 reflections were collected, of which 27637 reflections were independent ($R_{\text{int}} = 0.1056$). The structure was refined to final $R1 = 0.1177$ for 27637 data [$I > 2\sigma(I)$] with 2589 parameters, $wR2 = 0.3738$ for all data, $GOF = 0.757$, and residual electron density $\text{max./min.} = 0.656/-0.380 \text{ e}\cdot\text{\AA}^{-3}$. The ORTEP drawing is shown in Figure S19, and the crystal data and structure refinement are listed in Table S1.

Data collection, indexing, and initial cell refinements were carried out using the program SMART.^[5] Frame integration and final cell refinements were performed using SAINT software.^[6] A multiple absorption correction for each data set was applied using the program SADABS.^[7] The structure was solved by direct methods and Fourier techniques using the program SHELXS-97^[8] and refined by full-matrix least squares methods on F^2 using SHELXL-97^[9] incorporated in SHELXTL-PC.^[1] All non-hydrogen atoms were refined anisotropically. Hydrogen atoms were fixed at calculated positions and refined using a riding model. The water hydrogen atoms were not located because they have disordered configurations.

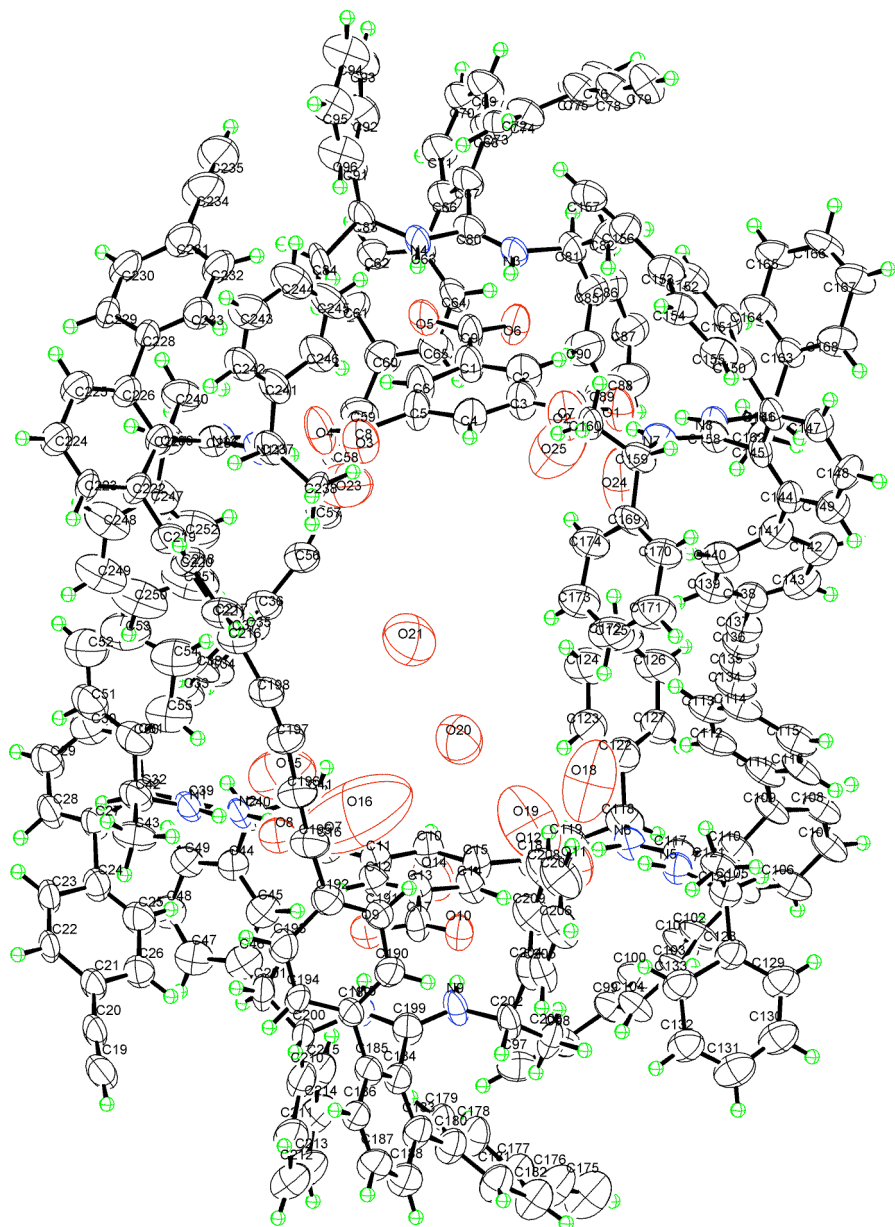


Figure S19. An ORTEP drawing of the crystal structure of the [3+2]cylindrical complex (S)-3 with thermal ellipsoids at 50% probability.

Table S1. Crystal data and structure refinement for cylindrical complex (S)-3

Empirical formula	(C ₂₅₂ H ₁₉₈ N ₁₂ O ₁₂), 10(H ₂ O)	
Formula weight	3766.57	
Temperature	153 K	
Wavelength	0.71073 Å	
Crystal system	<i>Triclinic</i>	
Space group	<i>P1</i>	
Unit cell dimensions	<i>a</i> = 17.395(2) Å	α = 88.211(2)°
	<i>b</i> = 18.235(3) Å	β = 87.456(3)°
	<i>c</i> = 22.228(3) Å	γ = 63.587(3)°
Volume	6307.9(15) Å ³	
<i>Z</i>	1	
Density (calculated)	0.993 Mg/m ³	
Absorption coefficient	0.063 mm ⁻¹	
<i>F</i> (000)	1970	
Crystal size	0.30 x 0.15 x 0.05 mm ³	
Theta range for data collection	2.17 to 25.35°	
Index ranges	-18<=h<=20, -21<=k<=21, -26<=l<=25	
Reflections collected	32965	
Independent reflections	27637 [R(int) = 0.1056]	
Completeness to theta = 25.35°	98.3%	
Absorption correction	Empirical	
Max. and min. transmission	0.9994 and 0.9814	
Refinement method	Full-matrix least-squares on F ²	
Data / restraints / parameters	27637 / 1927 / 2589	
Goodness-of-fit on F ²	0.757	
Final R indices [<i>I</i> >2sigma(<i>I</i>)]	<i>R</i> ₁ = 0.1177, <i>wR</i> ₂ = 0.2968	
R indices (all data)	<i>R</i> ₁ = 0.3472, <i>wR</i> ₂ = 0.3738	
Largest diff. peak and hole	0.656 and -0.380 e·Å ⁻³	

Absorption and CD Spectra of the [3+2]Cylindrical Complex (R)-3 at Various Temperatures

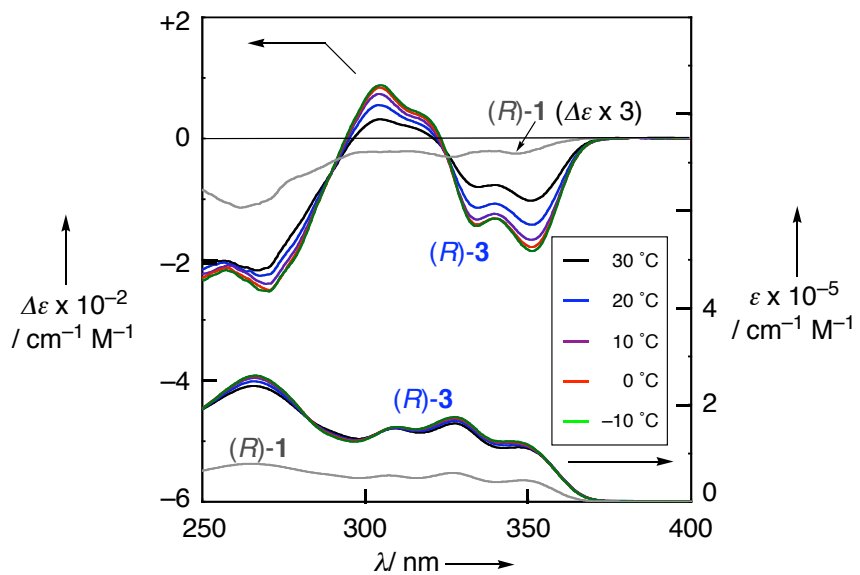


Figure S20. Absorption and CD spectra of (R)-3 (0.1 mM) at various temperatures.

Absorption and CD Spectra of the [4+2]Cylindrical Complex (R)-5 at Various Temperatures

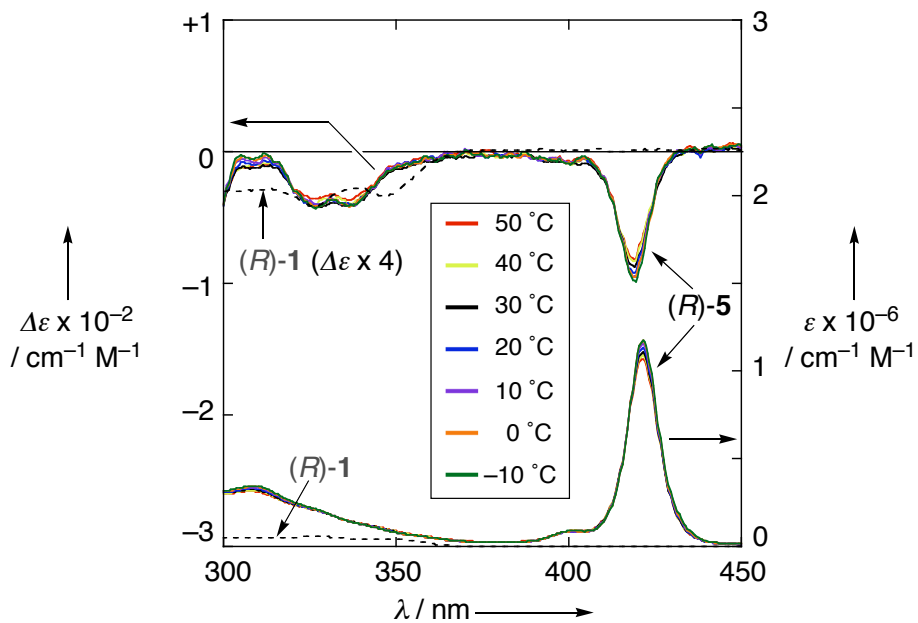


Figure S21. Absorption and CD spectra of (R)-5 (0.1 mM) at various temperatures.

Changes in the Absorption and CD Spectra of the [4+2]Cylindrical Complex (*R*)-5 upon Addition of Pyridine

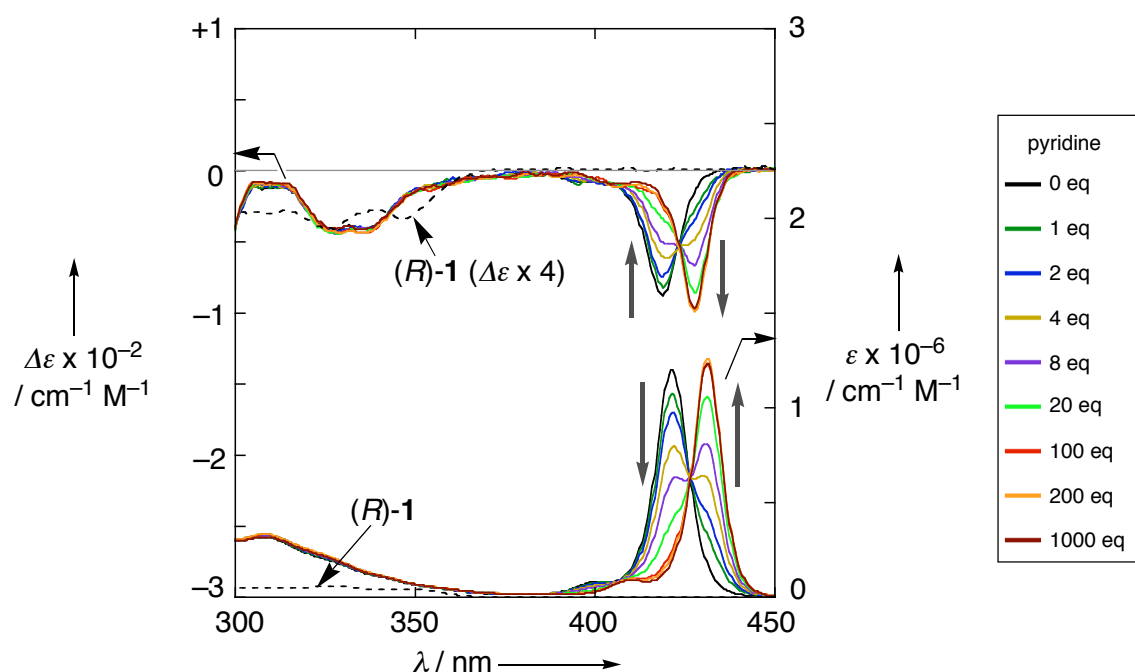


Figure S22. Changes in the absorption and CD spectra of (*R*)-5 in CDCl_3 (0.1 mM) upon addition of pyridine at 25 °C.

4. References

- [1] Bruker. SHELXTL Version 5.10: Suite of Programs for Crystal Structure Analysis, Incorporating Structure Solution (XS), Least-Squares Refinement (XL), and Graphics (XP); Bruker AXS, Inc., Madison, Wisconsin, USA (2000).
- [2] a) Y. Tanaka, H. Katagiri, Y. Furusho, E. Yashima *Angew. Chem.* **2005**, *117*, 3935–3938; *Angew. Chem. Int. Ed.* **2005**, *44*, 3867–3870; b) M. Ikeda, Y. Tanaka, T. Hasegawa, Y. Furusho, E. Yashima, *J. Am. Chem. Soc.* **2006**, *128*, 6806–6807.
- [3] A. Harada, K. Shiotsuki, H. Fukushima, H. Yamaguchi, M. Kamachi, *Inorg. Chem.* **1995**, *34*, 1070–1076.
- [4] K. Kobayashi, K. Ishii, S. Sakamoto, T. Shirasaka, K. Yamaguchi, *J. Am. Chem. Soc.* **2003**, *125*, 10615–10624.
- [5] Bruker. SMART Version 5.624: Program for collecting frames of data, indexing reflection, and determination of lattice parameters; Bruker AXS, Inc., Madison, Wisconsin, USA (2000).
- [6] Bruker. SAINT Version 6.02: Program for integration of the intensity of reflections and scaling; Bruker AXS, Inc., Madison, Wisconsin, USA (2000).
- [7] G. M. Sheldrick, SADABS Version 2.03: Program for Performing Absorption Corrections to Single-Crystal X-ray Diffraction Patterns; University of Göttingen, Göttingen, Germany (2001).
- [8] G. M. Sheldrick, SHELXS-97: Program for the Solution of Crystal Structures; University of Göttingen, Göttingen, Germany (1997).
- [9] G. M. Sheldrick, SHELXL-97: Program for the Refinement of Crystal Structures; University of Göttingen, Göttingen, Germany (1997).